Autoionization spectra of Sm atom*

Zhao Yan-Hong(赵艳红)[a)b)], Dai Chang-Jian(戴长建)[a)b)†], and Ye Shi-Wei(野仕伟)[a)b)]

[a)] *Key Laboratory of Display Materials and Photoelectric Devices, Ministry of Education, Tianjin* 300384, *China*
[b)] *School of Science, Tianjin University of Technology, Tianjin* 300384, *China*

(Received 3 July 2012; revised manuscript received 5 September 2012)

Spectra of autoionizing states of the Sm atom in an energy region between 45948.9 cm^{-1} and 46943.6 cm^{-1} are systematically investigated by a three-color multi-step resonant excitation scheme with three different excitation paths. The three intermediate states, $4f^6 6s7s\ ^7F_3$, $4f^6 6s7s\ ^7F_4$, and $4f^6 6s7s\ ^9F_5$ are employed for the three paths, respectively. Based on precise calibration of wavelength, the level energies of 112 autoionizing states are determined with the line widths and the relative line intensities of the related transitions. The possible influence of configuration interaction on the line shape of autoionizing state is also discussed. In addition, a unique value of J, the total angular momentum, is assigned to all detected states by comparing the three spectra obtained with the different excitation paths.

Keywords: Sm atom, autoionizing state, three-color multi-step resonant excitation

PACS: 32.70.Jz, 32.70.FW, 32.80.DZ **DOI:** 10.1088/1674-1056/22/2/023203

1. Introduction

Investigations on autoionizing atoms not only reveal their inner structures and the coupling effect from electron–electron or electron–ion, but also become an alternative approach to understanding the mechanism of the dielectronic recombination,[1–4] which is a reverse process of autoionization. In addition, it can play an important role in laser isotope separation and the development of new lasers, lasers without population inversion. Due to the development of tunable dye lasers and the multi-step laser excitation scheme, the autoionizing states of alkaline-earth atoms have been studied widely in the last two decades.[5,6] However, the study of autoionizing states of rare-earth atoms is still scanty.[7–10]

The spectra of rare-earth atoms are usually very complex due to the fact that the 4f shell is only partially filled for these atoms except Yb. Among the rare-earth atoms, the Yb atom[11,12] has been studied most due to the fact that the 4f shell is completely filled. However, in the case of the Sm atom, with an unstable shell consisting of six 4f electrons, the spectrum is much more complex since they are formed by transitions of the electrons from both the outer $6s^2$ electrons and the inner $4f^6$ electrons. In addition, the ground terms of the Sm atom include ground state $4f^6 6s^2\ \ ^7F_0$ and the six metastable states $4f^6 6s^2\ \ ^7F_J$ ($J = 1$–6), while the ground term of the Yb atom has only one ground state. Since the ground terms lie in an energy range of 0 cm^{-1}–4021 cm^{-1}, they are readily populated thermally when the Sm metal sample is heated.[13] For instance, at 800 K, the thermal populations of the above seven states are 21.03% ($^7F_0$), 37.83% ($^7F_1$), 25.45% ($^7F_2$), 10.98% ($^7F_3$), 5.55% ($^7F_4$), 0.99% ($^7F_5$), and 0.25% ($^7F_6$), respectively. Meanwhile, unlike the Yb atom which has only one $6s^+$ ionization limit, the Sm atom possesses 12 additional $6s^+$ ionization limits, which lie in an energy range of 327 cm^{-1}–5318 cm^{-1} above the first $6s^+$ ionization limit. The technical challenges in carrying out the experiments caused by the above properties are obvious: (i) the signals from a given initial state are much weaker; (ii) a photon may drive several transitions originating from different excitation schemes; (iii) there are many autoionization series converging to the 12 different $6s^+$ ionization limits. Thus, precautions must be taken to achieve the goals, such as the discrimination of the unexpected transitions, and the identification of autoionizing states, since the studies on the odd-parity autoionizing states of the Sm atom are mainly in the region above 4.88×10^4 cm^{-1},[14–17] below which few investigations have been carried out.[18,19] With all the facts in mind, the present work will systematically study the spectra of the odd-parity autoionizing states in an energy region between 45948.9 cm^{-1} and 46943.6 cm^{-1} with a three-color resonant excitation scheme, in order to obtain their level energies, relative line intensities of the related transitions, and unique J-assignment. In addition, the possible influences of the configuration interaction on the properties of autoionization spectrum, such as line width and line shape, will also be discussed.

In the following text, an introduction of experimental details will be presented in Section 2; the experimental results and relevant discussion will be given in Section 3; in Section 4 some conclusions will be drawn from the present study.

*Project supported by the National Natural Science Foundation of China (Grant Nos. 11174218 and 10674102) and the Natural Science Foundation of Tianjin, China (Grant No. 05YFJMJC05200).

†Corresponding author. E-mail: daicj@126.com

© 2013 Chinese Physical Society and IOP Publishing Ltd

2. Experiment

The experimental setup is comprised of three parts: a laser system, an atomic beam and ion-detection system, and a data acquisition system. A schematic diagram of the experimental setup is illustrated in Fig. 1.

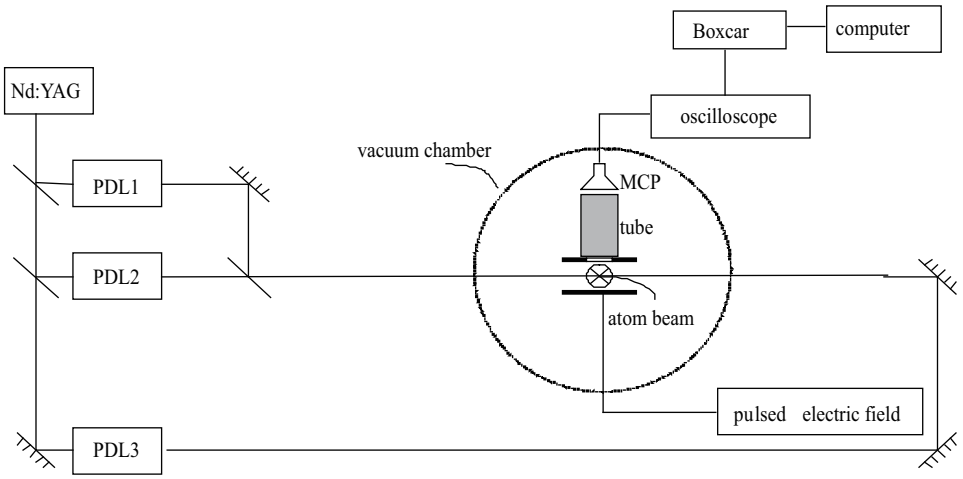


Fig. 1. Schematic diagram of the experimental setup. It includes the laser system, the atomic beam and ion-detection system, and the data acquisition system.

Specifically, the laser system consists of an Nd:YAG pulsed laser and three tunable dye lasers, each of which has a pulse width of 5 ns–8 ns, and is running at a frequency of 20 Hz. The tunable dye lasers are pumped by the second or third harmonic generation (SHG or THG) of Nd:YAG pulsed laser, each of which has a line width of 0.1 cm^{-1}. The pulses of the second and third lasers are delayed by 10 ns and 20 ns relative to the pulse of the first laser, respectively, so that three laser pulses are sequential in time.

The atomic beam and ion-detection system is enclosed in a vacuum chamber, in which it comprises an atomic oven with a beam collimator, and a micro-channel plate (MCP) ion detector. The Sm atomic beam sprays from a resistively heated oven maintained at 800 K, which is collimated and directed to a region between two electric field plates, 1 cm apart, where it is crossed perpendicularly by the laser beams to avoid the Doppler broadening. About 500 ns after the laser pulses, a pulsed electric field of 50 V/cm is applied to the plates in order to drive the ions resulting from the excitation and subsequent decay of autoionizing states into an MCP detector, so as to avoid the Stark effect in the spectrum. The time delay mentioned above is controlled by a digital pulse generator.

The data acquisition system includes a Boxcar, a digital oscilloscope, and a computer with a data-collection software, Acquire. The ions are detected by the MCP detector whose signal is monitored with a digital oscilloscope, and integrated and averaged by the Boxcar, of which the output is digitized with an A–D convertor, and stored in a computer for further analysis.

In order to ensure the accuracy of experimental data on level energy, both systematic and random errors in the wavelength of scanning laser need to be minimized. For instance, the wavelength of the dye laser is absolutely calibrated with the optogalvanic spectra of hollow-cathode lamps, whose spectral lines are known accurately. It is also relatively calibrated by the spectrum of a Fabry–Perot etalon, which can correct the nonlinearity in each scan. Moreover, to reduce the random errors in the spectra, each spectrum is the average of those measured several times. With all efforts mentioned above, the present work can provide the level energies within an accuracy of about 0.2 cm^{-1}.

Since the measured spectra are expected to provide the information about the level energy, relative line intensity, line width as well as the J-assignment, several different excitation paths need to be designed to ensure the effective schemes for detecting the autoionizing states. The selection rules of all relevant transitions should enable us to assign a unique J value by combining the spectra obtained with different excitation paths in the same energy region. Accordingly, the Sm atom is excited to the autoionizing states via the following three paths:

$$\text{I}\ \ 4f^6 6s^2\ {}^7F_1 \xrightarrow{\lambda_1=678.10\ \text{nm}} 4f^6 6s6p\ {}^9D_2 \xrightarrow{\lambda_2=636.31\ \text{nm}} 4f^6 6s7s\ {}^7F_3 \xrightarrow{\lambda_3} E_J\ (J=2,3,4),$$

$$\text{II}\ \ 4f^6 6s^2\ {}^7F_2 \xrightarrow{\lambda_1=680.48\ \text{nm}} 4f^6 6s6p\ {}^9D_3 \xrightarrow{\lambda_2=624.97\ \text{nm}} 4f^6 6s7s\ {}^7F_4 \xrightarrow{\lambda_3} E_J,\ (J=3,4,5),$$

$$\text{III}\ \ 4f^6 6s^2\ {}^7F_3 \xrightarrow{\lambda_1=709.74\ \text{nm}} 4f^6 6s6p\ {}^9G_4 \xrightarrow{\lambda_2=651.77\ \text{nm}} 4f^6 6s7s\ {}^9F_5 \xrightarrow{\lambda_3} E_J,\ (J=4,5,6).$$

The above three paths are apparently three-color multistep resonant $\lambda_1+\lambda_2+\lambda_3$ excitation processes, an example of which is shown in Fig. 2(a). It is worth noting that the thermal populations in the seven fine structures of the ground state may cause two serious consequences in

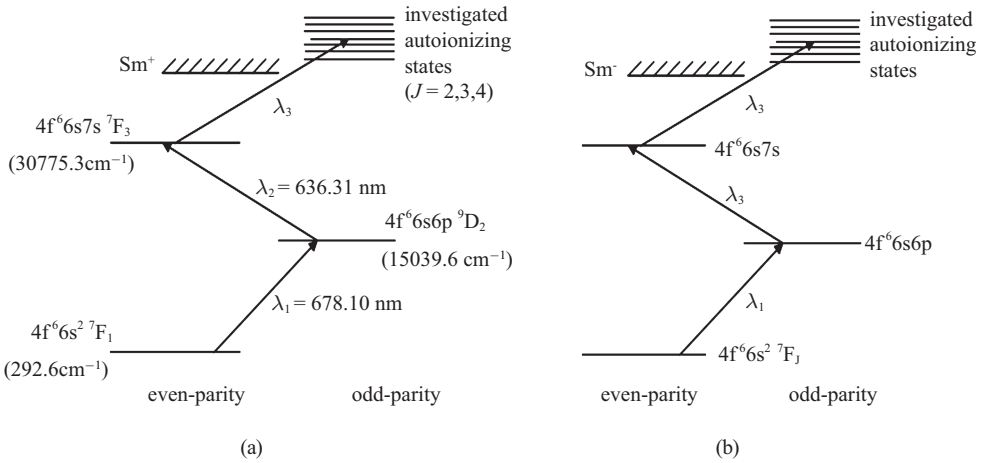


Fig. 2. Excitation schemes used in the experiment: (a) three-color multi-step $\lambda_1+\lambda_2+\lambda_3$ process; (b) two-color three-step $\lambda_1+\lambda_3+\lambda_3$ process.

the $\lambda_1+\lambda_2+\lambda_3$ process: firstly, the number of atoms in a given initial state is reduced significantly, thus weakening the line intensity of the transition; secondly, signals from two-color multi-step $\lambda_1+\lambda_3+\lambda_3$ excitation process as shown in Fig. 2(b), may disturb the desired $\lambda_1+\lambda_2+\lambda_3$ process.

In order to discriminate the unexpected signals, it is necessary to make comparisons between the two cases where spectra are obtained in the presence and the absence of the λ_2 photon, while λ_3 is scanned within the same region. Based on the above comparison, it is easy to indicate which state belongs to the $\lambda_1+\lambda_3+\lambda_3$ process.

As shown in Fig. 2(a), the Sm atom in the initial state $4f^6 6s^2\ ^7F_1$ is excited to the $4f^6 6s6p\ ^9D_2$ intermediate state by the first laser with a wavelength of $\lambda_1 = 678.71$ nm, from which it is excited to the $4f^6 6s7s\ ^7F_3$ Rydberg state by the second laser with a wavelength of $\lambda_2 = 636.71$ nm, then the Sm atom is excited further to the autoionizing states with $J = 2, 3,$ and 4 by scanning the wavelength λ_3 of the third laser. Finally, the Sm atom in the autoionizing state may automatically decay into an ion and an electron, which can be detected as the autoionization process. Similarly, for the path II, the $4f^6 6s7s\ ^7F_4$ Rydberg state is used, which can be excited with the two photons of $\lambda_1 = 680.48$ nm and$\lambda_2 = 624.97$ nm, and the final states with $J = 3$, 4, and 5 are related. For the path III, the $4f^6 6s7s\ ^7F_5$ Rydberg state is used, which can be excited with the two photons of $\lambda_1 = 709.74$ nm and $\lambda_2 = 651.77$ nm, while the final states with $J = 4$, 5, and 6 are involved.

For all the excitation paths described, the energy of the observed autoionizing state can be obtained by the relation $E = E_{6s7s} + hc/\lambda_3$, where E_{6s7s} is the energy of the $4f^6 6s7s$ Rydberg state excited by the first two photons, and λ_3 is the wavelength of the third laser at the peak position of the autoionization spectrum.

In addition to determining the level energies of the autoionizing states, their total angular momentum J can also be assigned uniquely by comparing the spectra obtained with different excitation paths in the same energy region. Namely, the comparison of spectra obtained with the three paths will yield five unique assignments: i) if a transition can only be observed in the spectra obtained with path I, then it can be assigned with $J = 2$; ii) if a transition can be observed in the spectra obtained with path I and path II but not in that obtained with path III, then it can be assigned with $J = 3$; iii) if a transition can be observed in the spectra obtained with the three paths, it can be assigned with $J = 4$; iv) if a transition can be observed in the spectra obtained with path II and path III, but not in that obtained with path I, then it can be assigned with $J = 5$; v) if a transition can only be observed in the spectra obtained with path III, then it can be assigned with $J = 6$.

3. Results and discussion

As mentioned above, 112 autoionizing states in the energy region between 45948.9 cm^{-1} and 46943.6 cm^{-1} are measured systematically in this work. To our knowledge, 107 of these autoionizing states have not been observed previously. An example of many observed autoionization spectra in an energy region between 46240 cm^{-1} and 46360 cm^{-1} is shown in Fig. 3, which are obtained with the path I.

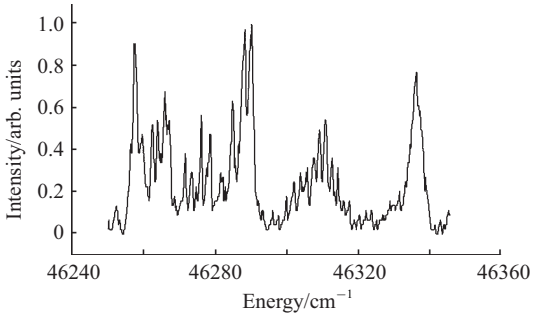


Fig. 3. Experimental spectrum of the Sm autoionizing Rydberg states obtained with path I.

As shown in Fig. 3, many autoionzating states have various line widths and line shapes. From a spectroscopic point of view, an autoionizing state is a quasi-bound state whose width

represents the total autoionization rate to all possible underlying continua, and reflects its coupling strength with them. For an independent autoionzation Rydberg series, the widths of many autoionizing states in the same series should be scaled as n^{-3}, where n is the principal quantum number of the Rydberg series. However, it is by no means an independent autoionzation Rydberg series due to the multi-limit problem, which leads to the complicated features on the line shape of any autoionizing state.

To explain this phenomenon, one should keep the following facts in mind: the number of the $6s^+$ ionization limits is greater than 10, to which many autoionzation Rydberg series are converged. Due to the configuration interaction among many autoionization series and relevant continuum, there are two effects on the autoionization spectrum: a) the width of the autoionizing state is changed significantly with energy, but does not obey the n^{-3} law; b) there are many complicated structures in the autoionization spectrum: several narrow peaks overlap with a broad profile as can be seen from Fig. 3.

Although it is impossible for us to classify these autoionizing states into the specific ionization limits, some suggestions can still be made: the broader peak represents the lower-n member of the autoionization series converging to the higher ionization limit, while the peak with much smaller width is related to the higher-n member converging to the lower ionization limit.

Since the autoionizing states reported here are related to many ionization limits, some information may be deduced from their line shapes. As shown in Fig. 3, the observed spectra exhibit many nearly symmetric line shapes of the autoionizing states, indicating a little interference between the excitations to the autoionizing states and the continuum states, similar to those obtained from the isolated core excitation,[20] which has been proven to be an advanced excitation scheme in studying spectra of autoionizing states.[21,22]

With the above analysis in mind, the observed profile of an autoionizing state may be simplified from the Fano line shape[23] into the Lorentzian line shape, corresponding to the case where the Fano q parameter is much greater than one. Accordingly, as a standard treatment, both the level energy and the width of autoionizing state can be obtained by fitting the experimental spectra to the Lorentzian profiles as shown in Fig. 4. The uncertainties of both energy and width can be improved by fitting the observed spectra to the Lorentzian line shape compared with by reading directly from the observed spectra, especially for the case where the signal-to-noise ratio is not good enough.

As an example, figure 4 shows the result of fitting with the Lorentz profile for the autoionizing state with the greatest line width in Fig. 3. The solid line represents the experimental spectrum, and the dashed line is from the best fit of the Lorentzian profile. The positions and width of this autoionizing state are 46309.8 cm^{-1} and 6.5 cm^{-1}, respectively.

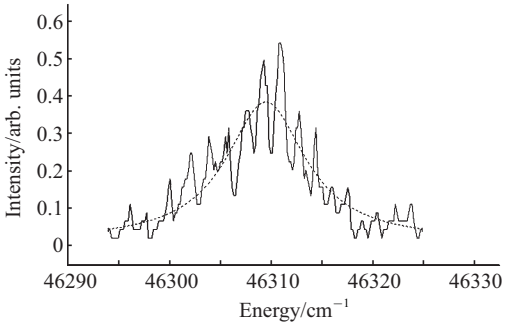


Fig. 4. Fitting result from the Lorentzian profile. The solid line represents the experimental spectrum of the Sm atom, while the dashed line is from the fitting procedure.

The sharp features in the spectrum are the fingerprints of interseries interaction between the two autoionization series converging to the two different ionization limits. The main profile in Fig. 4 reflects the autoionizing state converging to the higher limit, which has a larger width due to its lower n value, while the sharp features are the autoionizing states converging to the lower limit, with a much smaller width due to their higher n value. On the other hand, the autoionizing state with a width of 6.5 cm^{-1} implies its weak interaction with the continuum states, leading to a smaller autoionization rate.

Figure 5 displays another example, which is obtained with the path II in an energy region between 46650 cm^{-1} and 46900 cm^{-1}.

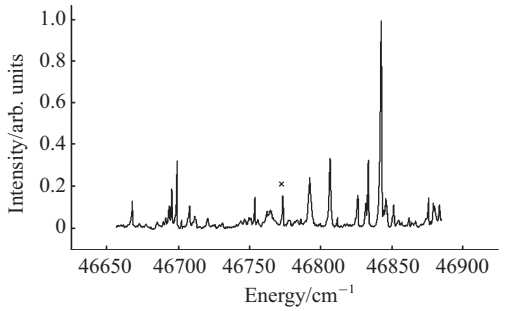


Fig. 5. Autoionization spectrum of the Sm atom observed with path II.

As shown in Fig. 5, the transition marked with "×" sign originates from the $\lambda_1 + \lambda_3 + \lambda_3$ ($\lambda_1 = 709.74$ nm, $\lambda_3 = 630.85$ nm) process as shown in Fig. 2(b). In the present work, 9 similar transitions are found with $\lambda_1 = 709.74$ nm, $\lambda_3 = 659.99$ nm and $\lambda_1 = 678.10$ nm, $\lambda_3 = 621.90$ nm, 625.41 nm, 625.42 nm, 630.63 nm, 630.84 nm, 633.74 nm, 634.94 nm, 637.30 nm, 640.86 nm respectively. The interference of these transitions has been eliminated with the method described in Section 2.

With the same procedures as those used in Figs. 3 and 5, all the experimental spectra are analyzed, from which the spectroscopic information about 112 autoionizing states, including their level energies, relative line intensities, line widths, and unique J-assignment, is given as shown in Table 1–3. In order to make different transitions comparable, their relative line intensities are normalized to one, and the letters W (weak), M (medium), and S (strong) are used to represent the intensities from 0 to 0.3, from 0.4 to 0.6 and from 0.7 to 1, respectively.

Now we come to pay our attention to the spectroscopic information about the 38 autoionizing states with $J = 2$ shown in Table 1.

Table 1. Autoionizing states of the Sm atom with $J = 2$. The information about their level energies, line widths, and relative line intensities is given.

Serial number	Energy/cm^{-1}	Line width/cm^{-1}	Relative intensity	Serial number	Energy/cm^{-1}	Line width/cm^{-1}	Relative intensity
1	46046.5	3.0	S	20	46542.00	4.2	M
2	46058.7	5.8	M	21	46573.5	4.1	S
#3	46083.1	1.1	W	22	46647.3	3.0	S
4	46094.9	0.7	S	23	46679.1	2.7	W
5	46109.7	2.8	M	24	46685.5	1.1	W
#6	46128.0	1.4	M	25	46718.4	3.0	M
7	46148.0	0.7	M	26	46726.1	3.7	M
8	46165.8	2.7	S	27	46745.8	12.6	S
#9	46194.1	1.0	W	28	46778.1	3.0	S
10	46203.9	0.9	S	29	46786.1	0.9	M
#11	46212.6	3.2	S	30	46792.9	4.8	M
12	46229.8	0.8	M	31	46800.8	1.5	M
#13	46263.0	15.3	M	32	46815.2	1.7	M
14	46288.7	4.4	S	33	46828.4	2.6	W
15	46309.8	6.5	M	34	46870.8	3.6	W
16	46336.4	3.6	S	35	46891.4	7.3	M
17	46428.2	2.6	M	36	46909.2	4.1	M
18	46460.9	2.0	S	37	46909.2	4.1	M
19	46467.9	2.9	S	38	46938.3	7.1	M

The autoionizing states whose level energies confirm the previous results.

Table 2. Autoionizing states of the Sm atom with $J = 3$, 4, and 5. The information about their level energies, line widths, relative line intensities, and the unique J-assignment is given.

Serial number	Energy/cm^{-1}	Line width/cm^{-1}	Relative intensity	J	Serial number	Energy/cm^{-1}	Line width/cm^{-1})	Relative intensity	J
1	46088.9	1.7	M	3	22	46765.1	4.3	M	4
2	46120.0	1.2	S	3	23	46845.6	1.4	W	4
3	46131.8	1.0	M	3	24	46850.8	2.0	M	4
4	46134.3	1.1	M	3	25	46879.8	1.8	M	4
5	46157.5	2.3	M	3	26	46883.3	1.2	W	4
6	46533.7	1.3	S	3	27	46902.0	1.6	M	4
7	46665.7	1.4	W	3	28	46111.4	0.9	M	5
8	46706.9	1.3	M	3	29	46191.9	0.9	M	5
9	46709.7	2.1	M	3	30	46514.1	6.3	M	5
10	46819.4	3.9	M	3	31	46606.4	2.0	S	5
11	46106.4	1.7	M	4	32	46648.2	2.5	M	5
12	46142.1	2.3	S	4	33	46678.4	1.9	W	5
13	46224.9	1.0	W	4	34	46707.9	1.0	M	5
14	46438.6	1.5	W	4	35	46720.6	1.5	M	5
15	46457.2	1.1	M	4	36	46731.1	2.1	M	5
16	46465.2	1.4	M	4	37	46791.2	2.8	M	5
17	46552.6	4.5	M	4	38	46806.8	1.6	M	5
18	46583.5	4.1	M	4	39	46811.4	1.1	W	5
19	46589.8	1.8	M	4	40	46875.3	1.4	W	5
20	46631.3	1.2	M	4	41	46940.4	1.0	W	5
21	46711.3	2.1	W	4					

Table 3. Autoionizing states of the Sm atom with $J = 6$. The information about their level energies, line widths, and relative line intensities is given.

Serial number	Energy/cm^{-1}	Line width/cm^{-1}	Relative intensity	Serial number	Energy/cm^{-1}	Line width/cm^{-1}	Relative intensity
1	45948.9	2.2	M	18	46487.4	1.0	S
2	45991.9	1.1	M	19	46490.6	1.2	W
3	46019.3	2.0	W	20	46511.4	0.7	M
4	46086.5	1.4	S	21	46516.4	0.7	W
5	46118.5	1.3	S	22	46565.4	2.1	W
6	46199.1	1.2	S	23	46595.6	1.2	W
7	46295.1	0.8	W	24	46635.4	0.9	W
8	46322.3	0.8	W	25	46656.8	1.6	S
9	46337.5	0.7	W	26	46695.7	0.9	W
10	46382.3	1.0	W	27	46699.2	0.7	M
11	46387.1	1.1	S	28	46753.5	0.7	W
12	46398.7	1.0	W	29	46832.7	0.7	M
13	46406.2	1.0	S	30	46842.1	1.3	S
14	46416.8	0.8	S	31	46913.1	0.7	W
15	46440.3	1.3	W	32	46922.3	0.7	S
16	46445.7	0.7	M	33	46943.6	1.3	M
17	46471.2	1.0	S				

As shown in Table 1, not only their level energies and line widths are obtained by fitting the experimental spectra to the Lorentzian profiles, but also a unique J-assignment is given to all the autoionizing states by comparing the spectra obtained with the three paths. Among these states, level energies of five autoionizing states, marked with the symbol '#', confirm the previous results by adding the information about the line width, the relative line intensity, and a unique J-assignment.

Turning now to Table 2, where 10 autoionizing states with $J = 3$, 17 autoionizing states with $J = 4$, and 14 autoionizing states with $J = 5$ are reported. Moreover, the information about their level energies, the line widths, and relative intensities of related transitions is also given in the present work.

From the comparison with Table 1, it can be seen that the relative line intensities of the $J = 2$ autoionizing states are stronger than those with $J = 3$, 4 or 5. In other words, for the $J = 2$ autoionizing states there are more states with relative line intensities of S than for other J value autoionizing states. The possible reason is that the values of transition probability to the autoionizing states with $J = 3$, 4 or 5 are much less than those with the $J = 2$ autoionizing states.

Similarly, the $J = 6$ autoionizing states can be determined with the same method described in Section 2. The information about these states is provided in Table 3 for the first time.

As shown in Table 3, one may find the following facts: 1) the number of $J = 6$ states is almost the same as that of $J = 2$ states; 2) the number of $J = 6$ states is much smaller than those of $J = 3$, 4 and 5 states. The possible reasons are that the relative line intensities of the $J = 6$ states are generally stronger than those of $J = 3$, 4 or 5 states. Note that the spectral information about the $J = 6$ states is reported for the first time.

4. Conclusion

Using the three-color multi-step resonant excitation method, the spectra of autoionizing states of the Sm atom are systematically studied. Three excitation paths are used to observe 112 autoionizing states in the energy region between 45948.9 cm^{-1} and 46943.6 cm^{-1}. The present work not only provides the information about their energies, line widths, and relative line intensities, but also unambiguously assigns the angular momentum J to all the observed autoionizing states. In addition, the possible influences of the configuration interaction on the properties of the autoionization spectrum, such as line width and line shape, are also discussed.

References

[1] Korol A V, Gribakin G F and Currell F J 2006 *Phys. Rev. Lett.* **97** 1
[2] Zhao Z X and Brabec T 2006 *J. Phys.* B: *At. Mol. Opt. Phys.* **39** L345
[3] Zhang H, Li Y M, Yan J and Wang J G 2005 *Phys. Rev.* A **71** 042705
[4] Rosmej F B 2006 *Europhys. Lett.* **76** 1081
[5] Li S B and Dai C J 2003 *J. Quantum Spectrosc. Radia. Transfer* **77** 345
[6] Dai C J and Li S Ben 2007 *Chin. Phys.* **16** 382
[7] Zhong Y P, Jia F D and Zhong Z P 2009 *Chin. Phys.* B **18** 4242
[8] Li M, Dai C J and Xie J C 2011 *Chin. Phys.* B **20** 063204
[9] Jayasekharan T, Razvi M A N and Bhale G L 2000 *J. Phys.* B: *At. Mol. Opt. Phys.* **33** 3123
[10] Xiao Y, Dai C J and Qin W J 2010 *Chin. Phys.* B **19** 063202
[11] Yi J H and Lee J M 1994 *Phys. Rev.* A **51** 3053
[12] Ali R, Yaseen M and Nadeem A 1999 *J. Phys.* B: *At. Mol. Opt. Phys.* **32** 953
[13] Jayasekharan T, Razvi M A N and Bhale G L 2000 *J. Opt. Soc. Am.* B **17** 1607
[14] Qin W J, Dai C J and Xiao Y 2010 *J. Quantum Spectrosc. Radiat. Transfer* **111** 63

[15] Qin W J, Dai C J and Xiao Y and Zhao H Y 2009 *Chin. Phys.* B **18** 1833

[16] Qin W J, Dai C J and Xiao Y 2010 *J. Quantum Spectrosc. Radiat. Transfer* **111** 997

[17] Park Hyunmin, Kim Hyun-Chae, Yi Jonghoon, Han Jaemin, Rhee Yong-Joo and Lee Jongmin 1998 *Journal of the Korean Physical Society* **33** 288

[18] Hu S F, Zhang S, Mei S M, Qiu J Z and Chen X 1990 *J. Quantum Spectrosc. Radiat. Transfer* **43** 75

[19] Hu S F, Mei S M and Zhang S 1989 *Chin. Phys. Lett.* **6** 64

[20] Cooke W E, Gallagher T F and Edelstein S A 1978 *Phys. Rev. Lett.* **20** 178

[21] Dai C J and Schinn G W 1990 *Phys. Rev.* A **42** 223

[22] Li S B, Dai C J and Sun W 2001 *J. Phys.* B **34** 981

[23] Fano U 1961 *Phys. Rev.* **124** 1866